

# Analysis and Optimization of Monolithic Inductors and Transformers for RF ICs

Ali M. Niknejad and Robert G. Meyer

Department of Electrical Engineering and Computer Science  
University of California at Berkeley  
Berkeley, CA 94720

## Abstract

A fast and accurate approach for analyzing Si IC spiral inductors and transformers is presented. The technique incorporates the substrate in the calculation to fully characterize the devices. Many test structures are fabricated and measured data is used to verify the analysis technique over a broad frequency range. Suitable lumped broadband equivalent circuit models of the structures are presented which can be incorporated into traditional circuit simulators. A custom CAD tool *ASITIC* is described which is used for the design and optimization of inductors and transformers.

## Introduction

Spiral inductors and transformers have the potential to improve the performance of key Si RF building blocks. Their use, though, has been hampered by the inability to model these structures over a wide frequency range due to the conductive nature of the Si substrate. Since the introduction of spiral inductors in silicon [1], much work has been done to improve the performance of these structures by optimizing the technology [2][3]. Little work, though, has been done in analyzing these structures. Past researchers have often opted for full 3D EM analysis, or the modeling has been semi-empirical, often curve-fitting key parameters requiring fabrication prior to modeling.

When analytic modeling has been done, the work has oversimplified the substrate impedance and coupling calculation. Often the measured Q factor or  $y_{21}$  is used to verify analytic models of the spirals. Although important performance factors, these parameters are not suitable for verifying the accuracy of analytic models. The Q factor is essentially a ratio, and errors often cancel.  $y_{21}$  is dominated by the inductance and series resistance of the spiral, and is very simple to calculate to first order. These parameters are not sensitive to accurate calculation of the substrate impedance. This is a problem since the substrate impedance and coupling play key roles in determining the performance of the devices. Hence, the proper modeling of the substrate is integral. In this paper we will present a general technique that yields the two-port parameters of any arbitrary arrangement of conductors over a multi-layer conductive substrate.

## Description of Technique

It can be shown that at frequencies of interest in RF ICs, the typical spiral inductor or transformer can be analyzed using

electrostatic and magnetostatic approximations. Even at 10 GHz, the time retardation of the potential across the length of a typical spiral, on the order of 100  $\mu\text{m}$ , is negligible. Furthermore, for the magnetostatic calculation the current flowing in the conductive segments is several orders of magnitude larger than the displacement and conductive currents flowing in the oxide and substrate layers. Hence, the magnetostatic calculation reduces to a free-space calculation, and for all practical purposes the substrate can be ignored for this calculation. If substrate current is on the order of the spiral current, then the analysis is more difficult. A mirror ground current approximation can be employed to greatly simplify the calculation [4]. This is usually not necessary, though, since even highly doped layers are much more resistive than the metal conductors. Even if the back plane is grounded, it is usually located very far from the spiral (300 $\mu\text{m}$  - 700 $\mu\text{m}$ ) and its effects are not substantial. Further, at high frequency, skin-effect in the bulk limits the substrate current to the surface of the substrate.

Therefore, to calculate the mutual and self inductance, the Geometric Mean Distance (GMD) approximation is appropriate and general formulas appear in [5] for various geometric configurations. To improve the approximation, and to include skin-effect and proximity effects, each conductor is further divided into parallel sub-conductors of constant current density. Using the technique and approximation in [6], this leads to a dense frequency-dependent mutual and self-inductance matrix  $Z_M$ . This matrix automatically takes skin-effect and proximity effects into account. Many past researchers [2][7] have used closed-form equations to approximate the skin effect. But such formulas only apply to isolated conductors, and the proximity of close conductors further influences the current distribution within each conductor. Since optimal spirals use very close spacing to maximize the Q of the inductor, it is important to include such proximity effects.

The electrostatic calculation is more complex since the substrate cannot be neglected. To calculate the electrostatic impedance matrix  $Z_C$  we use the method of moments [8]. Each metal segment of the spiral is subdivided into constant charge sections to accurately calculate the capacitance and resistance to the substrate, as well as to other metal segments. We use the semi-analytic approach of [9] to extract

## 16.3.1

**Table I** Qubic 2 BiCMOS Process Parameters

Layer	$\rho$ ( $\Omega$ -cm)	$\epsilon_r$	thickness ( $\mu\text{m}$ )
Substrate	15	11.9	650
Surface of Sub.	.075	11.9	1
Metal 1	50 $\Omega$ /sq	n.a.	1.0
Metal 2	32 $\Omega$ /sq	n.a.	1.3

the substrate impedance efficiently. Whereas in [9] the Green function is derived at the surface of a multi-layer substrate, we extend this work by deriving the Green function for an arbitrary location within the substrate. This allows metal-to-metal and metal-to-substrate impedance to be calculated. It is important to note that this technique can be used for any multi-layer substrate. This is important since the number of substrate layers, as well as their doping, will often vary from process to process. In addition, the substrate impedance is sensitive to the number and location of substrate-taps placed by the designer. This analysis takes these various factors into account.

Using the magnetostatic impedance matrix  $Z_M$  and the electrostatic impedance matrix  $Z_C$ , and assuming segments are connected in series<sup>1</sup>, we write  $2n$  nodal equations

$$\frac{V_j}{Z_{j0}^C} + \sum_{k \neq j} \frac{V_j}{Z_{jk}^C} - \sum_{k \neq j} \frac{V_k}{Z_{jk}^C} + I_j - I_{j-1} = 0 \quad (1)$$

$$V_j - V_{j+1} = \sum_k Z_{jk}^M I_k \quad (2)$$

where  $V_i$  is the voltage of the  $i$ th conductor segment, and  $I_i$  is the current through the  $i$ th conductor. The above system of equations can be inverted to find the  $y$ -parameters at any frequency of interest. Alternatively, each segment may be approximated by a two-port by first neglecting all coupling capacitance (off-diagonal terms of  $Z_C$ ) and then lumping each segment inductance and resistance by summing the rows of  $Z_M$ . This approximation holds at low-frequency when no current flows through the coupling capacitors. The resulting system may be simplified by cascading the  $n$  two-ports into a single two port model [10]. This approximation may be further refined by noting that

$$I_n = I - \sum_{i=1}^{n-1} \frac{V_i}{Z_{i0}^C} - \sum_{i=1}^{n-1} \sum_{j=n+1}^N \frac{V_i - V_j}{Z_{ij}^C} \quad (3)$$

where  $I$  is the total AC current injected into the spiral. By taking the appropriate weighted sum of the rows of  $Z_M$  according to (3), one can obtain a better estimate of the  $y$ -parameters. The unknown voltages may be approximated in an iterative fashion from the two-port matrix cascade calculation.

<sup>1</sup> Parallel segments are handled automatically in this technique since we start by subdividing each segment into parallel segments. Hence, this technique is also applicable to multi-metal layer inductors such as the ones appearing in [3].

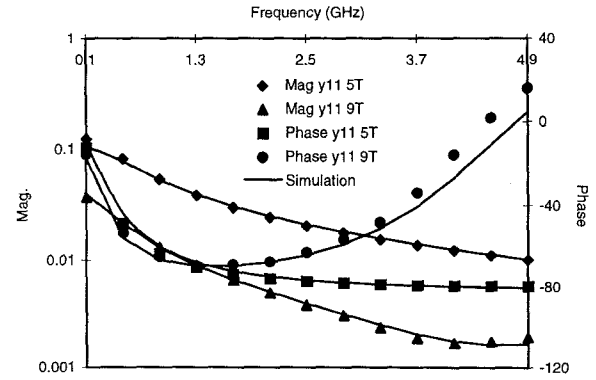


**Figure 1** Measured and simulated  $Y_{11}$  of square spirals.

### Measurement Results

To validate the above modeling technique, several spiral inductors and transformers were fabricated. We present a subset of the structures here. The Philips Qubic-2 BiCMOS process was used to fabricate the inductors. Approximate process parameters are shown in Table I. The inductors were placed on metal 2 and were connected to bonding pads. A substrate tap grounded the conductive surface of the Si substrate. Two-port  $s$ -parameters of the inductors and transformers were measured from 100MHz - 5GHz. Pad substrate impedance was de-embedded by subtracting out the open-circuit  $y$ -parameters from the spiral  $y$ -parameters. It is important to observe that this de-embedding procedure cannot cancel the substrate coupling that occurs between the pads and the inductor itself. We found it important to simulate the inductors in the same manner that we measured them (de-embedding bonding pads) in order to replicate this flaw in the procedure. At the same time, this tested our technique's ability to accurately extract substrate coupling that occurs between bond-pads.

We first examine the common and important square spiral inductor structure. Two example spirals are selected. Both have inner dimension of  $44\mu\text{m}$  and are wound with metal of

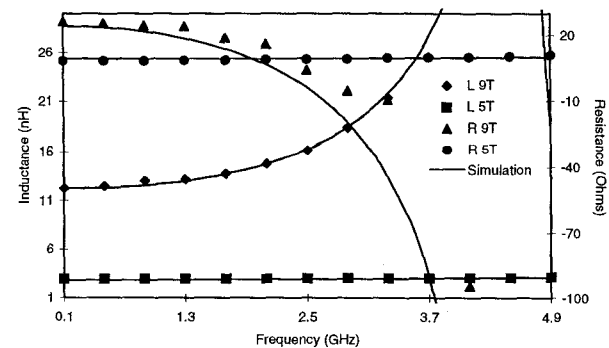


**Figure 2** Effective series resistance and inductance of square spirals.

## 16.3.2

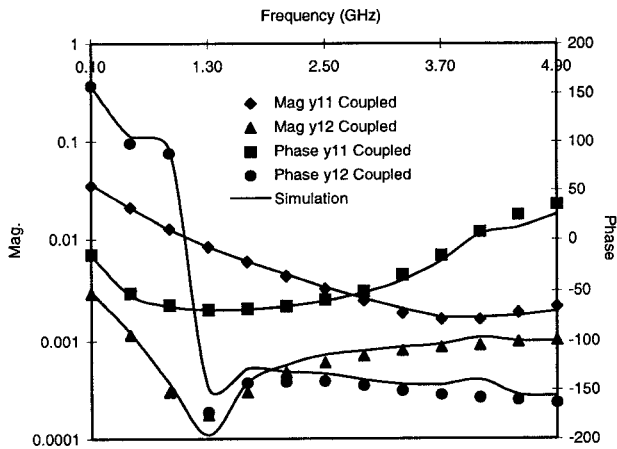


Figure 3 Measured and simulated y-parameters of coupled inductors.

width  $7\mu\text{m}$  and of spacing  $5\mu\text{m}$ . The first inductor has 5 turns, whereas the second has 9 turns. Metal 1 is used as the bridge layer to contact the inner turn of the spiral. Fig. 1 is a plot of the measured and simulated  $y_{11}$  of the two square spiral inductors.<sup>2</sup>

Effective series resistance and inductance can be extracted from the real and imaginary parts of  $y_{12}$ . These are plotted in Fig. 2. The inductance increases for both structures as a function of frequency, due to the bridging impedance and resonance behavior.<sup>3</sup> The resistance profile is influenced by the substrate impedance. Whereas lower substrate impedance tends to decrease the effective series resistance, the coupling impedance tends to increase the resistance. The resistance profile of the 5T spiral is dominated by coupling impedance whereas the profile of the 9T spiral is dominated by the low substrate impedance.

Many RF designs employ coupled inductors in differential stages. Hence, it is important to be able to model not only the magnetic coupling for a pair of spirals, but also the unwanted coupling through the substrate. In other cases, several inductors appear on the same IC and it is desirable to know the parasitic coupling. Two 9T square spirals similar in geometry to the aforementioned spiral were wound symmetrically and placed  $100\mu\text{m}$  apart. The resulting measured and simulated y-parameters are shown in Fig. 3. Good agreement is found for other separation distances as well.

Monolithic transformers also find many applications in a RF IC [7]. Their characterization is of utmost importance due to parasitic coupling between the two ports of the device.

<sup>2</sup>  $y_{12}$  is not plotted since there is no noticeable difference between measurement and simulation.

<sup>3</sup> There is actually a small underlying decrease in inductance as a function of frequency at increasingly higher frequency as the internal inductance decreases due to the skin effect.

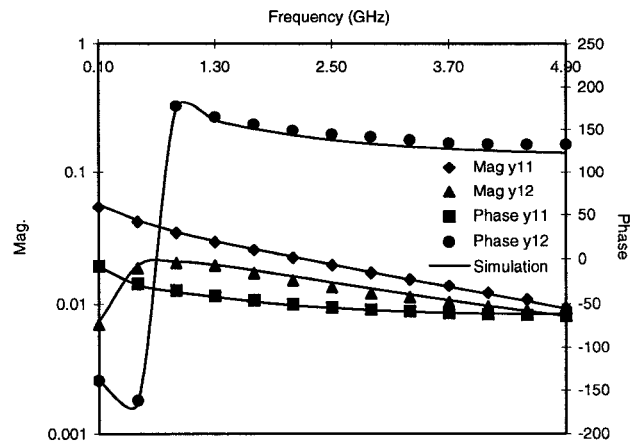


Figure 4 Measured and simulated y-parameters of transformer.

Hence, in addition to accurately predicting the coupling coefficient  $k$ , it is also important to predict the parasitic substrate coupling between the two ports. A test planar transformer was fabricated, consisting of two interwound 5 turn spiral inductors of width  $7\mu\text{m}$  and spacing  $12\mu\text{m}$  both of inner area  $44\mu\text{m}$ . The measured and simulated y-parameters for the test structure are shown in Fig. 4.

#### Lumped Equivalent Circuit Models

While the y-parameters generated in the previous section may be used directly in frequency domain analysis, it is convenient to use lumped circuit models to represent the behavior over a broad range appropriate in time domain simulations such as SPICE. Furthermore, lumped models often give the designer intuition as well as key parasitic parameters useful for design.

The circuit of Fig. 5 was first proposed by [2] to model the spiral inductor. The basic pi circuit of [1] is broadbanded by including a bridging capacitance. The value of the capacitance is not truly physical, but is more of an optimization parameter to fit the y-parameters of the lumped circuit to that of the actual y-parameters. Furthermore, substrate shunting capacitance and skin-effect were added to further improve the fit. For simple square spirals in our process, we found the simple pi circuit with a bridging capacitance to be sufficient.

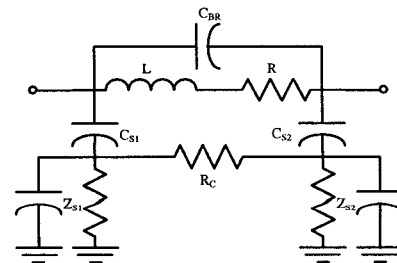


Figure 5 Lumped circuit model of spiral.

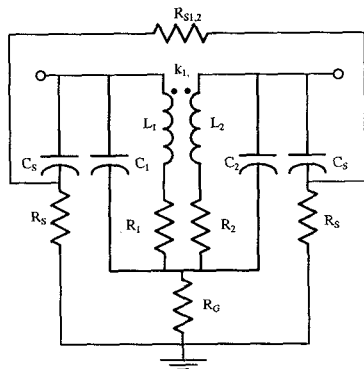


Figure 6 Lumped circuit model of coupled inductors.

For 9T coupled inductors, the circuit of Fig. 6 is used. This circuit is an extension of Fig. 5, where  $C$  is a lossless bridging capacitance for each structure,  $C_s$  and  $R_s$  model the substrate injection, and  $R_{s1,2}$  models the substrate coupling between the inductors.  $R_G$  is essential to match  $s_{21}$  at low frequency since this resistor represents an in-phase feedthrough. The coupling  $k$  models the mutual inductance between the spirals.

The transformers are modeled exactly like the coupled inductors, except a coupling capacitor  $C$  is added from input to output to model the coupling through the oxide between the input and output. As expected, the coupling factor  $k$  is much larger.

### Optimization

ASITIC is a custom CAD tool designed to aid in the optimization of spiral inductors and transformers [11]. The program takes in a set of electrical specifications such as desired inductance, resistance, self-resonance, and translates these specifications to a set of geometric parameters (spacing, width, area, geometry) to optimize a given parameter such as  $Q$ . The program can also work with an entire chip layout so that coupling between different inductors/transformers, as well as other metal structures, can be obtained.

In order to work quickly, the program searches through the parameter space using approximate calculations of the capacitance matrix  $Z_C$  and the inductance matrix  $Z_M$ . Many closed-form approximations exist [10] [12] to calculate the coupling and substrate capacitance in closed-form. In addition, the inductance matrix may be calculated quickly using the GMD approximation as before. In this way, the optimizer is fast and computationally efficient. As the optimizer limits the search space using these approximations, it then uses the more accurate technique described before to find the optimal solution.

### Conclusion

A general and accurate method appropriate for the analysis of spiral inductors and transformers, as well as other arrangement of metal conductors, has been presented. Its validity is tested against measurement results from a wide variety of structures. Lumped element equivalent circuits have been presented which model the device dynamics over a wide range of frequencies.

### Acknowledgments

The authors thank Bill Mack, Janice Eisenstadt, and Yen Nguyen of Philips for their help and support in fabricating and measuring the spirals. Also, the authors thank Ranjit Gharpurey of Texas Instruments for his valuable insights. This work was supported by the U.S. Army Research Office under Grant DAAH04-93-G-0200.

### References

- [1] N. M. Nguyen and R. G. Meyer, "Si IC-compatible inductors and LC passive filters," *IEEE J. Solid-State Circuits*, vol. 27, no. 10, pp. 1028-1031, Aug. 1990.
- [2] K. B. Ashby, W. C. Finley, J. J. Bastek, S. Moinian, and I. A. Koullias, "High Q inductors for wireless applications in a complementary silicon bipolar process," in *Proc. Bipolar and BiCMOS Circuits and Technol. Meet.*, Minneapolis, MN, 1994, pp. 179-182.
- [3] J. N. Burghartz, M. Soyuer, and K. Jenkins, "Microwave inductors and capacitors in standard multilevel interconnect silicon technology," *IEEE Trans. Microwave Theory Tech.*, vol. 44, no. 1, pp. 100-103, Jan. 1996.
- [4] D. Krafesik and D. Dawson, "A closed-form expression for representing the distributed nature of the spiral inductor," *Proc. IEEE-MTT Monolithic Circuits Symp. Dig.*, pp. 87-91, 1986.
- [5] F. W. Grover, *Inductance Calculations*. Princeton, N.J.: Van Nostrand, 1946, reprinted by Dover Publications, New York, 1954.
- [6] W. T. Weeks, L. L. Wu, M. F. McAllister, and A. Singh, "Resistive and inductive skin effect in rectangular conductors," *IBM J. Res. Develop.*, vol. 23, pp. 652-660, Nov. 1979.
- [7] J. R. Long and M. A. Copeland, "A 1.9 GHz low-voltage silicon bipolar receiver front-end for wireless personal communications systems," *IEEE J. Solid-State Circuits*, vol. 30, no. 12, Dec. 1995.
- [8] S. Ramo, J. R. Whinnery, and T. Van Duzer, *Fields and Waves In Communication Electronics*. 3<sup>rd</sup> ed., John-Wiley and Sons, Inc, 1994, pp. 324-330.
- [9] R. Gharpurey, R. G. Meyer, "Analysis and simulation of substrate coupling in integrated circuits," *IEEE J. Solid-State*, vol. 31, no. 3, pp. 344-53, March 1996.
- [10] E. Pettenpaul, H. Kapusta, A. Weisgerber, H. Mampe, J. Luginland, and I. Wolff, "CAD models of lumped elements on GaAs up to 18 GHz," *IEEE Trans. Microwave Theory Tech.*, vol. 36, no. 2, pp. 294-304, Feb. 1988.
- [11] ASITIC: *Analysis of Si Inductors and Transformers for ICs*, <http://www.eecs.berkeley.edu/~niknejad>.
- [12] R. Garg and I. J. Bahl, "Characteristics of coupled microstriplines," *IEEE Trans. Microwave Theory Tech.*, vol. MTT-27, pp. 700-705, 1979.